Responsive Supramolecular Polymer Metallogel Constructed by Orthogonal Coordination-Driven Self-Assembly and Host/Guest Interactions

Xuzhou Yan,[†] Timothy R. Cook,[‡] J. Bryant Pollock,[‡] Peifa Wei,[†] Yanyan Zhang,[∥] Yihua Yu,[∥] Feihe Huang,*,[†] and Peter J. Stang*,[‡]

[†]State Key Laboratory of Chemical Engineering, Department of Chemistry, Zhejiang University, Hangzhou, Zhejiang 310027, P. R. China

[‡]Department of Chemistry, University of Utah, 315 South 1400 East, Room 2020, Salt Lake City, Utah 84112, United States

[∥]Shanghai Key Laboratory of Magnetic Resonance, Department of Physics, East China Normal University, Shanghai 200062, P. R. China

Ⓢ *Supporting Information*

ABSTRACT: An emerging strategy for the fabrication of advanced supramolecular materials is the use of hierarchical self-assembly techniques wherein multiple orthogonal interactions between molecular precursors can produce new species with attractive properties. Herein, we unify the spontaneous formation of metal−ligand bonds with the host/guest chemistry of crown ethers to deliver a 3D supramolecular polymer network (SPN). Specifically, we have prepared a highly directional dipyridyl donor decorated with a benzo-21-crown-7 moiety that undergoes coordination-driven self-assembly with a complementary organoplatinum acceptor to furnish hexagonal metallacycles. These hexagons subsequently polymerize into a supramolecular network upon the addition of a bisammonium salt due to the formation of [2]pseudorotaxane linkages between the crown ether and ammonium moieties. At high concentrations, the resulting 3D SPN becomes a gel comprising many cross-linked metallohexagons. Notably, thermo- and cation-induced gel−sol transitions are found to be completely reversible, reflecting the dynamic and tunable nature of such supramolecular materials. As such, these results demonstrate the structural complexity that can be obtained when carefully controlling multiple interactions in a hierarchical fashion, in this case coordination and host/guest chemistry, and the interesting dynamic properties associated with the materials thus obtained.

The structural complexity and functional specificity demonstrated across multiple biological macromolecules provides inspiration for exploiting related hierarchical self-assembly methods to synthesize state-of-the-art supramolecular materials with dynamic and tunable properties.[1] One class of these materials are supramolecular gels constructed from low molecular weight precursors that can undergo intramolecular interactions to deliver extended molecule-based networks that oftentimes show stimuli-responsiveness, dynamic structural properties, and attractive characteristics for tissue engineering, drug-delivery, nanotechnology, etc.[2] When the molecular precursors used in gel formation possess internal cavities, the resulting gels may possess additional functionalities based on potential host/guest chemistry.[3] Existing examples of cavity-containing gelators are mainly based on traditional covalent macrocycles, such as cucurbit[n]urils, cyclodextrins, calixarenes, and so on.[4] These precursors are typically formed by grafting gelating moieties onto exiting covalent cores. An alternative approach is to organize the gelators using a preliminary self-assembly step, providing a facile route to metallacyclic cores that maintain an internal cavity and orient pendant groups with high directionality.[5]
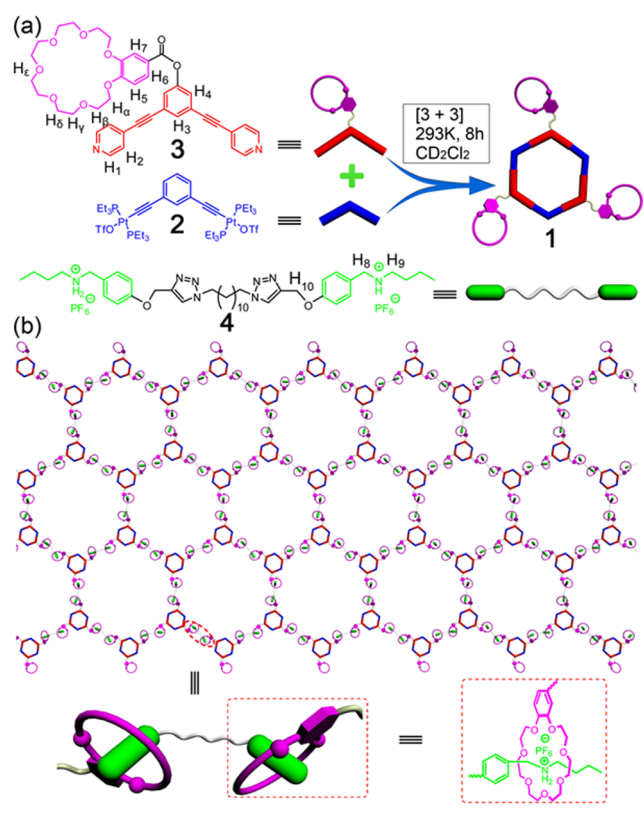
Coordination-driven self-assembly is a well-established method to construct supramolecular coordination complexes (SCCs) based on the spontaneous formation of metal−ligand bonds.[6] This approach organizes metal acceptors and organic donors to prepare well-defined metallacycles in which secondary recognition moieties can be easily functionalized.[7] Encouraged by the versatility and functionality of traditional cavity-containing gelators, we envisioned the preparation of gels based on the polymerization of metallacycles formed via an initial self-assembly step, wherein the desirable properties of the metallacyclic cores may be preserved in the final material.[3,8] However, metallacyclic gels based on well-defined discrete SCC cores have rarely been reported.

Crown ether-based host/guest interactions, which show good selectivity, high efficiency, and reversibility, have been widely employed in the construction of supramolecular polymeric materials.[9] When combined with coordination-driven assembly, remarkable supramolecular topological architectures can be prepared.[10] For example, the Stang group previously reported the formation of tris[2]pseudorotaxanes via metal-coordination and crown ether-based molecular recognition.[11] These examples demonstrate the use of secondary host/guest interactions in the formation of discrete supramolecular species. Herein, we unify the themes of host/guest interactions, coordination-driven self-assembly, and supramolecular polymerization through a hierarchical orthogonal design strategy to prepare a supra-

Scheme 1. (a) Self-Assembly of B21C7-Functionalized Discrete Metallacyclic Hexagon 1 and (b) Cartoon Representation of the Formation of a Cross-Linked 3D Supramolecular Polymeric Network from Self-Assembly of Hexagon 1 and Bisammonium Salt 4

Figure 1. Partial (a,b) ^{31}P and (c–e) ^{1}H NMR spectra (CD$_2$Cl$_2$, 293 K) of free building blocks **2** (a,e) and **3** (c), and hexagonal metallacycle **1** (b,d).

molecular metallogel containing hexagonal cavities in an extended network. A benzo-21-crown-7 (B21C7)-functionalized 120° dipyridyl ligand **3** self-assembles into a hexagonal metallacycle **1** when mixed with a 120° acceptor **2** (Scheme 1a). These discrete hexagons subsequently form the first example of a hexagonal-cored supramolecular polymer network (SPN) upon cross-linking the B21C7 moieties with a bisammonium salt **4** (Scheme 1b).The cross-linked material exhibits dynamic gel properties and sol−gel transitions based on temperature or the introduction of competing cations for the crown-ether sites.

The B21C7-functionalized ligand **3** was synthesized by an esterification reaction and a subsequent Pd-catalyzed Sonogashira coupling (Scheme S1). Stirring a mixture of ligand **3** and 1,3-bis[*trans*-Pt(PEt$_3$)$_2$(OTf)$_2$ ethynyl]benzene (**2**), in a 1:1 molar ratio in CD$_2$Cl$_2$ at room temperature for 8 h resulted in the formation of self-assembled [3 + 3] hexagon **1** with pendent B21C7 moieties at the vertices (Scheme 1a). Multinuclear NMR (^{1}H and ^{31}P) analysis of the reaction mixture supported the formation of a discrete, highly symmetric entity (Figure 1). The ^{31}P{^{1}H} NMR spectrum of **1** shows a sharp singlet at δ = 15.91 ppm with concomitant ^{195}Pt satellites corresponding to a single phosphorus environment (Figure 1, spectrum b). This peak is shifted upfield from acceptor **2** by ca. 6.10 ppm. In addition, in the ^{1}H NMR spectrum of **1** (Figure 1, spectrum d), the protons of the pyridyl groups showed downfield shifts ($\Delta\delta[H_1]$ = 0.04 ppm; $\Delta\delta[H_2]$ = 0.41 ppm) compared to those of ligand **3** (Figure 1, spectrum c), consistent with coordination of the *N*-atoms to platinum centers.
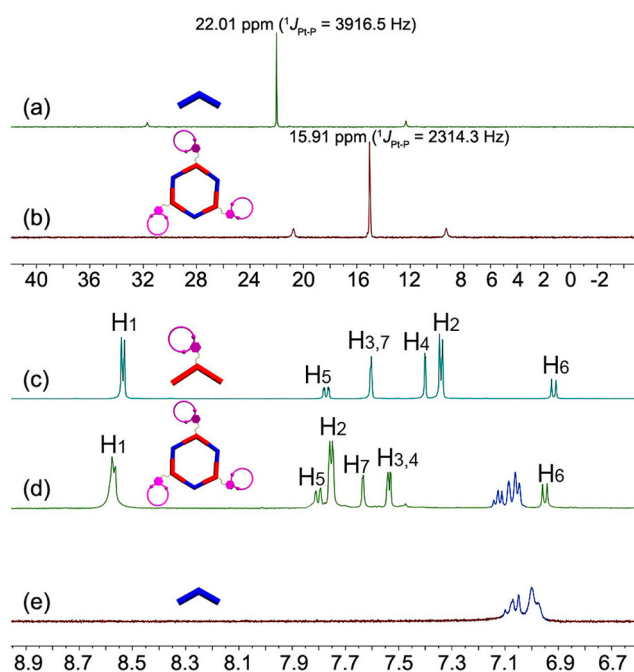
The formation of hexagonal metallacycle **1** was further confirmed by electrospray ionization time-of-flight mass spectrometry (ESI-TOF-MS). In the mass spectrum of **1**, six peaks were identified to support the formation of a [3 + 3] assembly (Figure S9), including those corresponding to an intact hexagonal core with charge states arising from the loss of counterions [m/z = 1323.66 for [M − 4OTf]$^{4+}$ (Figure 2a), m/z = 1029.14 for [M − 5OTf]$^{5+}$ (Figure 2b), and m/z = 832.79 for [M − 6OTf]$^{6+}$ (Figure 2c)]. All the peaks were isotopically resolved and in excellent agreement with their calculated theoretical distributions. PM6 semiempirical molecular orbital
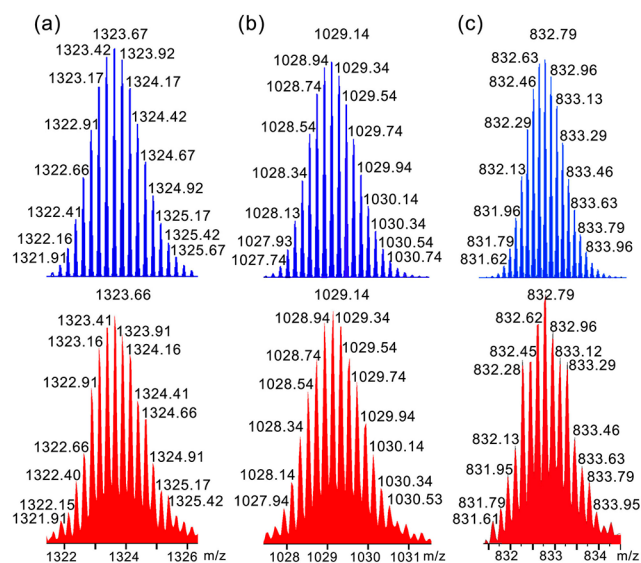

Figure 2. Experimental (red) and calculated (blue) ESI-TOF-MS spectra of hexagon **1**: (a) [M − 4OTf]$^{4+}$, (b) [M − 5OTf]$^{5+}$, and (c) [M − 6OTf]$^{6+}$.
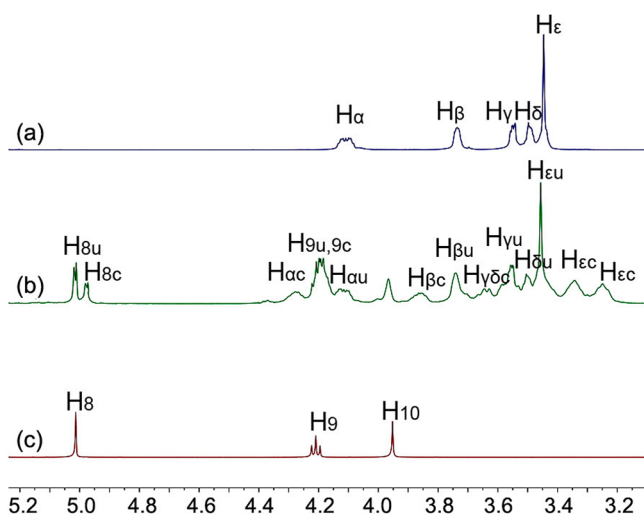
Figure 3. Partial ^{1}H NMR spectra [CD$_2$Cl$_2$/CD$_3$CN (1:1 v/v), 293 K, 500 MHz]: (a) B21C7-functionalized hexagon **1**; (b) a mixture of hexagon **1** and bisammonium salt **4** (6.00 mM crown ether/ammonium salt moieties); and (c) bisammonium salt **4**. Here "c" and "u" denote complexed and uncomplexed moieties, respectively.

Figure 4. (a) Concentration dependence of diffusion coefficient D [CD$_2$Cl$_2$/CD$_3$CN (1:1 v/v), 308 K, 500 MHz] of SPN. (b) Size distributions of SPN at different concentrations. (c) Rheological characterization (T = 278 K) of cavity-containing SPN metallogel. (d) Size distributions of SPN before and after addition of KPF$_6$ (peak A is DB18C6⊃K$^+$ and peak B is bisammonium salt **4**).

Figure 5. Formation of the cavity-containing SPN metallogel and its dual-responsive gel−sol transitions.

methods were used to obtain further insight into the structural characteristics of **1**. Simulations indicated a planar hexagonal framework with exohedral functionalization by the pendent B21C7 units and an internal diameter of 2.90 nm (Figure S10).

Proton ^{1}H NMR experiments provided important insight into the complexation behavior of hexagon **1** and bisammonium salt **4** in solution. Comparisons of the ^{1}H NMR spectra of hexagon **1**, bisammonium salt **4**, and their mixture, reveal chemical shift changes (Figure 3). As shown in Figure 3b, the ^{1}H NMR spectrum of the mixture is complicated and each of the protons of the B21C7 and ammonium units are split into two sets of signals, corresponding to the complexed and uncomplexed species, due to the slow-exchange nature of host/guest complexation relative to the proton NMR time scale.[12] Downfield chemical shift changes were observed for ethylenoxy protons H$_\alpha$, H$_\beta$, H$_\gamma$, and H$_\delta$, while methylene protons H$_8$ and H$_9$ and ethylenoxy protons H$_\varepsilon$ shifted upfield after complexation, in agreement with the well-known B21C7/dialkylammonium complexation motif.[13] These changes in chemical shifts indicated that B21C7/ammonium salt complexation exists in the cross-linked SPN, providing the intramolecular interactions necessary for mixtures of **1** and **4** to exhibit gel properties at high concentrations. The formation of an extended hexagonal network upon host/guest interactions between **1** and **4** was further investigated by concentration-dependent ^{1}H NMR experiments (Figure S11).

To further confirm SPN formation, 2D diffusion-ordered ^{1}H NMR spectroscopy (DOSY)[14] was performed to investigate the self-aggregation between hexagon **1** and bisammonium salt **4**. As the concentration of B21C7/ammonium salt units increased from 12.0 to 60.0 mM, the measured weight average diffusion coefficient decreased from 1.48×10^{-10} to 1.51×10^{-11} m^2 s^{-1} ($D_{12.0\text{mM}}/D_{60.0\text{mM}} = 9.80$) (Figure 4a), indicating the formation of a high molecular weight SPN. The DOSY NMR experiments were performed at 308 K because the SPN formed a gel in the concentration range of 35.0−60.0 mM at 293 K. Moreover, dynamic light scattering (DLS) measurements were conducted to study the size distributions of the SPN at different concentrations. As the concentration of the B21C7/ammonium
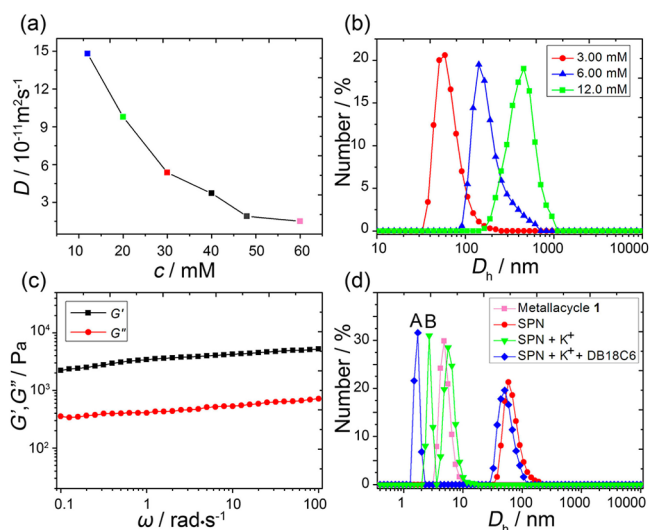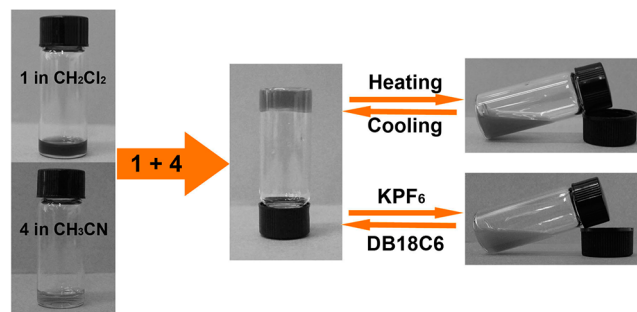
salt units in the SPN increased from 3.00 to 6.00 to 12.0 mM, the average hydrodynamic diameter (D_h) increased from 58.8 to 142 to 459 nm, indicating a concentration dependence on SPN size (Figure 4b).

Next, the gelation properties of the SPN were studied. Solutions of hexagon **1** in CH$_2$Cl$_2$ (60.0 mM B21C7 units) and bisammonium salt **4** in CH$_3$CN (60.0 mM ammonium salt moieties) were prepared in two vials (Figure 5, left). Upon addition of the bisammonium salt **4** solution into the solution of **1**, the hexagonal cavity-cored SPN metallogel was formed immediately (Figure 5, middle). This mixture contains 30.0 mM B21C7/ammonium moieties. The good association between B21C7 and ammonium moieties leads to the formation of extended hexagonal networks and a dramatic increase of viscosity, responsible for the observed gelation. The critical gel concentration was determined to be 20.0 mM B21C7/ammonium units at 4 °C.

Rheological characterization can give further insight to the bulk material properties of the cross-linked supramolecular assemblies. Therefore, a rheological analysis was carried out on the gel at a concentration of 40.0 mM B21C7/ammonium salt moieties at 278 K. The data revealed that the storage modulus (G') is much larger than the loss modulus (G''), and both of them (G' and G'') are independent of the angular frequency (ω),

thereby showing the formation of the hexagonal cavity-cored SPN metallogel (Figure 4c). Moreover, the morphology of the xerogel, prepared by a freeze-drying method, was examined by scanning electron microscopy (SEM), which revealed extended and interconnected fibers (Figure S12). As shown in Figure S12, the thin and long fibers can further self-organize into 2D ribbon-like fibrous structures that extend for several micrometers.

The reversible thermo- and cation-induced gel−sol transitions can be visualized macroscopically (Figure 5, middle and right). Qualitative characterization of the thermo-induced reversibility of this metallogel is demonstrated with an inverted vial test. Upon heating, the gel easily flows as the host/guest association constant decreases at elevated temperatures, indicating a gel−sol transition. This process is completely reversible as the gel reforms upon cooling due to the restoration of host/guest interactions. Moreover, the B21C7 moiety preferentially forms a 1:1 complex with potassium cation (K^+),[12] which provides a route for deconstructing the B21C7/ammonium linkages. Adding and removing K^+ can trigger reversible gel−sol conversions. DLS measurements showed that the addition of KPF_6 into a 3.00 mM B21C7/ammonium salt solution results in a decrease of the average D_h from 58.8 to 5.62 nm, indicating that the host/guest complexation is quenched. After addition of enough dibenzo-18-crown-6 (DB18C6) to trap all the K^+, the B21C7/ammonium complex is re-formed, and the average D_h recovers (Figure 4d). These reversible conversions can also be monitored by ^1H NMR experiments (Figure S13).

In summary, a B21C7-functionalized hexagonal metallacycle was prepared with high efficiency by means of the *directional-bonding approach*. This macrocyclic precursor could be extended into a supramolecular polymer upon the formation of [2]-pseudorotaxane host/guest linkages with a bisammonium salt. The gel that resulted from high concentrations of this supramolecular polymer exhibited dynamic properties, specifically thermo- and cation-induced sol−gel transitions. As this design method preserves internal metallacyclic cavities through the resulting SPN, such gels are promising candidates for applications in catalysis, separation, absorption, etc. Moreover, due to the stimuli-responsive nature of non-covalent interactions, the SPN gel can also act as a degradable material triggered by external stimuli. The design principles established here encompass hierarchical orthogonal self-assembly with coordination-driven self-assembly, host/guest interactions, and supramolecular polymerization. Given the rich chemistry of supramolecular coordination complexes and the favorable properties of emerging supramolecular polymers developed previously,[1c,7] the unification of metal−ligand coordination with orthogonal non-covalent interactions is a promising route to access novel supramolecular polymers with fascinating characteristics. Further efforts to organize non-covalent interactions between pendant-functionalized metallacycles are ongoing.

ASSOCIATED CONTENT

Ⓢ Supporting Information

Experimental details and additional data. This material is available free of charge via the Internet at http://pubs.acs.org.

AUTHOR INFORMATION

Corresponding Author

fhuang@zju.edu.cn; stang@chem.utah.edu

Notes

The authors declare no competing financial interest.

REFERENCES

(1) (a) Zimmerman, S. C.; Zeng, F.; Reichert, D. E. C.; Kolotuchin, S. V. *Science* **1996**, *271*, 1095. (b) Castellano, R. K.; Clark, R.; Craig, S. L.; Nuckolls, C.; Rebek, J., Jr. *Proc. Natl. Acad. Sci. U.S.A.* **2000**, *97*, 12418. (c) Yan, X.; Wang, F.; Zheng, B.; Huang, F. *Chem. Soc. Rev.* **2012**, *41*, 6042. (d) Lehn, J.-M. *Angew. Chem., Int. Ed.* **2013**, *52*, 2836. (e) Zhang, J.; Li, Q.; Hu, Q.; Wu, Q.; Li, C.; Qiu, H.; Zhang, M.; Yin, S. *Chem. Commun.* **2014**, *50*, 722.

(2) (a) Zhang, S.; Greenfield, M. A.; Mata, A.; Palmer, L. C.; Bitton, R.; Mantei, J. R.; Aparicio, C.; de la Cruz, M. O.; Stupp, S. I. *Nat. Mater.* **2010**, *9*, 594. (b) Yan, X.; Xu, D.; Chi, X.; Chen, J.; Dong, S.; Ding, X.; Yu, Y.; Huang, F. *Adv. Mater.* **2012**, *24*, 362. (c) Hisamatsu, Y.; Banerjee, S.; Avinashi, M. B.; Govindaraju, T.; Schmuck, C. *Angew. Chem., Int. Ed.* **2013**, *52*, 12550.

(3) Foster, J. A.; Steed, J. W. *Angew. Chem., Int. Ed.* **2010**, *49*, 6718.

(4) (a) Hwang, I.; Jeon, W. S.; Kim, H.-J.; Kim, D.; Kim, H.; Selvapalam, N.; Fujiata, N.; Shinkai, S.; Kim, K. *Angew. Chem., Int. Ed.* **2007**, *46*, 210. (b) Liu, Y.; Yu, Y.; Gao, J.; Wang, Z.; Zhang, X. *Angew. Chem., Int. Ed.* **2010**, *49*, 6576. (c) Appel, E. A.; del Barrio, J.; Loh, X. J.; Scherman, O. A. *Chem. Soc. Rev.* **2012**, *41*, 6195.

(5) Zhao, G.-Z.; Chen, L.-J.; Wang, W.; Zhang, J.; Yang, G.; Wang, D.-X.; Yu, Y.; Yang, H.-B. *Chem.—Eur. J.* **2013**, *19*, 10094. (b) Yan, X.; Li, S.; Cook, T. R.; Ji, X.; Yao, Y.; Pollock, J. B.; Shi, Y.; Yu, G.; Li, J.; Huang, F.; Stang, P. J. *J. Am. Chem. Soc.* **2013**, *135*, 14036.

(6) (a) Fujita, M.; Tominaga, M.; Hori, A.; Therrien, B. *Acc. Chem. Res.* **2005**, *38*, 369. (b) Gianneschi, N. C.; Masar, M. S., III; Mirkin, C. A. *Acc. Chem. Res.* **2005**, *38*, 825. (c) Oliveri, C. G.; Ulmann, P. A.; Wiester, M. J.; Mirkin, C. A. *Acc. Chem. Res.* **2008**, *41*, 1618. (d) Cook, T. R.; Zheng, Y.-R.; Stang, P. J. *Chem. Rev.* **2013**, *113*, 734. (e) Yan, X.; Li, S.; Pollock, J. B.; Cook, T. R.; Chen, J.; Zhang, Y.; Ji, X.; Yu, Y.; Huang, F.; Stang, P. J. *Proc. Natl. Acad. Sci. U.S.A.* **2013**, *110*, 15585. (f) Cook, T. R.; Vajpayee, V.; Lee, M. H.; Stang, P. J.; Chi, K.-W. *Acc. Chem. Res.* **2013**, *46*, 2464.

(7) (a) Chakrabarty, R.; Mukherjee, P. S.; Stang, P. J. *Chem. Rev.* **2011**, *111*, 6810. (b) Yan, X.; Jiang, B.; Cook, T. R.; Zhang, Y.; Li, J.; Yu, Y.; Huang, F.; Yang, H.-B.; Stang, P. J. *J. Am. Chem. Soc.* **2013**, *135*, 16813. (c) Leininger, S.; Olenyuk, B.; Stang, P. J. *Chem. Rev.* **2000**, *100*, 853. (d) Stang, P. J.; Olenyuk, B. *Acc. Chem. Res.* **1997**, *30*, 502.

(8) Tam, A. Y.-Y.; Yam, V. W.-W. *Chem. Soc. Rev.* **2013**, *42*, 1540.

(9) (a) Yamaguchi, N.; Nagvekar, D. S.; Gibson, H. W. *Angew. Chem., Int. Ed.* **1998**, *37*, 2361. (b) Gibson, H. W.; Yamaguchi, N.; Jones, J. W. *J. Am. Chem. Soc.* **2003**, *125*, 3522. (c) Huang, F.; Gibson, H. W. *J. Am. Chem. Soc.* **2004**, *126*, 14738. (d) Niu, Z.; Huang, F.; Gibson, H. W. *J. Am. Chem. Soc.* **2011**, *133*, 2836. (e) Avestro, A.-J.; Belowich, M. E.; Stoddart, J. F. *Chem. Soc. Rev.* **2012**, *41*, 5881. (f) Ji, X.; Yao, Y.; Li, J.; Yan, X.; Huang, F. *J. Am. Chem. Soc.* **2013**, *135*, 74.

(10) (a) Wang, F.; Zhang, J.; Ding, X.; Dong, S.; Liu, M.; Zheng, B.; Li, S.; Wu, L.; Yu, Y.; Gibson, H. W.; Huang, F. *Angew. Chem., Int. Ed.* **2010**, *49*, 1090. (b) Li, S.; Huang, J.; Cook, T. R.; Pollock, J. B.; Kim, H.; Chi, K.-W.; Stang, P. J. *J. Am. Chem. Soc.* **2013**, *135*, 2084.

(11) Yang, H.-B.; Ghosh, K.; Northrop, B. H.; Zheng, Y.-R.; Lyndon, M. M.; Muddiman, D. C.; Stang, P. J. *J. Am. Chem. Soc.* **2007**, *129*, 14187.

(12) Yan, X.; Xu, D.; Chen, J.; Zhang, M.; Hu, B.; Yu, Y.; Huang, F. *Polym. Chem.* **2013**, *4*, 3312.

(13) (a) Zhang, C.; Li, S.; Zhang, J.; Zhu, K.; Li, N.; Huang, F. *Org. Lett.* **2007**, *9*, 5553. (b) Yan, X.; Zhou, M.; Chen, J.; Chi, X.; Dong, S.; Zhang, M.; Ding, X.; Yu, Y.; Shao, S.; Huang, F. *Chem. Commun.* **2011**, *47*, 7086.

(14) (a) de Greef, T. F. A.; Ercolani, G.; Ligthart, G. B. W. L.; Meijer, E. W.; Sijbesma, R. P. *J. Am. Chem. Soc.* **2008**, *130*, 13755. (b) Xu, J.-F.; Chen, Y.-Z.; Wu, D.; Wu, L.-Z.; Tung, C.-H.; Yang, Q.-Z. *Angew. Chem., Int. Ed.* **2013**, *52*, 9738.